

## E-27 THE FLUID FACTOR ANGLE

MAURICE GIDLOW and GEORGE CAMERON SMITH

*PGS Geophysical, Cape Town. Department of Geological Sciences, University of Cape Town.*

### Introduction

Amplitude-versus-offset (AVO) procedures commonly used today are made up essentially of three steps. The first step is the estimation of two parameters, usually either the intercept and gradient terms, or scaled versions of compressional and shear reflectivity. The second step is the measurement of the general temporal and spatial variation of the relationship between these two parameters. This slowly varying relationship we call the background trend. The final step is the display of the data with this background trend removed. This display we call the Fluid Factor. It aims to produce interpreter sections whose amplitude is close to zero everywhere, except at the top and base of hydrocarbon bearing zones.

Another AVO attribute used widely is the far angle stack. Qualitatively it has been shown that in many instances this is a very successful hydrocarbon indicator. In this paper we show, using the concept of the Fluid Factor Angle, the equivalence between the far angle stack, the Fluid Factor section (Smith and Gidlow, 1987), and the Elastic Impedance section (Connolly, 1999).

### Discussion

An approximation to the Zoeppritz equation which we will use for this discussion is that of Shuey (1985), which describes the variation of compressional reflectivity  $R$  with angle of incidence  $\theta$  by:  $R = A + B \sin^2 \theta$ , where the intercept  $A$  and gradient  $B$  are determined by performing a least squares fit of this equation to the amplitudes in an NMO corrected CMP gather. The calculation of  $A$  and  $B$  is equivalent to making two weighted stacks.

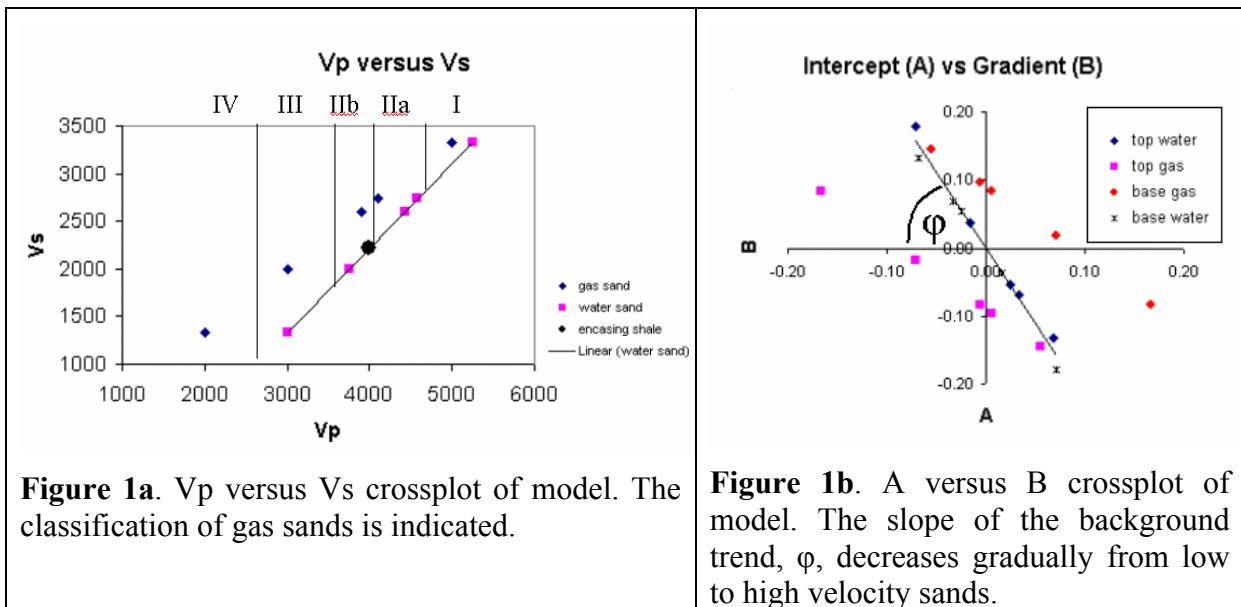
While the parameters  $A$  and  $B$  (or alternatively scaled compressional and shear reflectivities) on their own do not say a whole lot about the presence of hydrocarbons, combinations of them do. A simplified crossplot of compressional and shear velocities (or impedances, since density has been assumed constant for this simple example) is shown in figure 1a. The shales and water bearing sands fall on a linear trend called the mudrock line (Castagna, 1985). Gas sands exhibit an "upper-leftish" movement away from this trend, as do oil sands but to a lesser degree. Castagna and Smith (1994) published a world-wide set of data points that show this same trend. It is this trend of water sands and shales which we call the background trend, and it is the separation from this trend which we are attempting to measure and display in our AVO procedures.

Since the seismic experiment records the strength of reflections, our analysis takes place in reflectivity space rather than impedance space. The only significant difference between the Fluid Factor method and the Elastic Impedance method is that in the latter the analysis is performed in impedance space. This means that an inversion must be performed on the data prior to AVO analysis.

A simple model has been generated to explain the concept. The parameters are shown in Table 1. A shale overlies i) a gas filled sand, and ii) a water filled sand. For the purposes of explanation and simplification, constant density has been assumed.

AVO Type	Vp gas	Vs gas	Vp water	A gas	B gas	A water	B water
		<b>Vs water</b>					
<b>4</b>	2000	1333	3000	-0.17	0.08	-0.07	0.18
<b>3</b>	3000	2000	3750	-0.07	-0.02	-0.02	0.04
<b>2b</b>	3900	2600	4425	-0.01	-0.08	0.03	-0.05
<b>2a</b>	4100	2733	4575	0.01	-0.10	0.03	-0.07
<b>1</b>	5000	3333	5250	0.06	-0.14	0.07	-0.13
<b>Shale</b>		2222	4000				

**Table 1. Model parameters:** velocities of gas- and water-bearing sands and shale in m/s. A and B for shale over gas- or water-bearing sands. Constant density assumed.

$$A = \frac{1}{2} \frac{V_{p2} - V_{p1}}{V_{p2} + V_{p1}}, \quad B = A - \frac{V_{s2} - V_{s1}}{V_{s2} + V_{s1}}$$


### Crossplot Angle

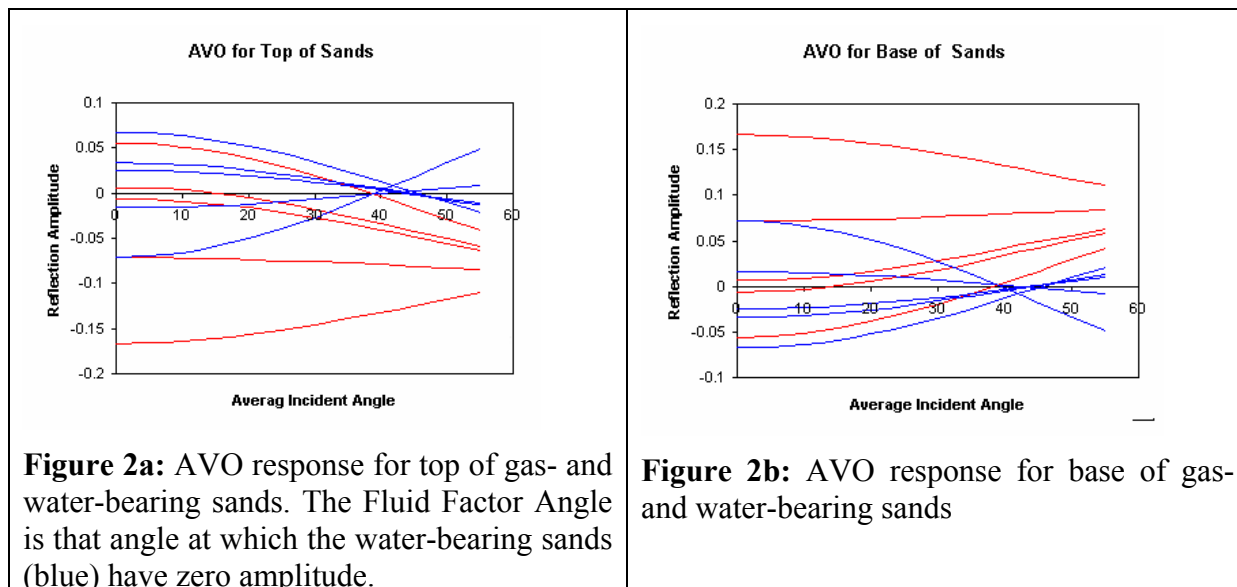
Figure 1a is a crossplot of the velocities, and figure 1b is a typical crossplot of intercept A versus gradient B. A background can be defined on figure 1b by a line best fitting the top and base water sand points. The angle between the horizontal intercept axis and this background line is here named phi ( $\phi$ ). The Fluid Factor trace can be envisaged as a measure of the distance of each sample point (A, B) from the background line. Close inspection of figure 1b reveals that the best background trend will actually be defined by a slowly rotating line with  $\phi$  gradually decreasing from low velocity sands (shallow) to high velocity sands (deep). Since the Fluid Factor is a combination of A and B which will produce a zero result for the background trend, and since  $\tan \phi = -B/A$  for the background trend, then the Fluid Factor may be defined as:

$$\text{Fluid Factor} = A \sin \phi + B \cos \phi$$

Inspection of figure 1b reveals that the Fluid Factor is negative at the top of gas-bearing sands and positive at the bottom.

## Fluid Factor Angle

Figures 2a and 2b show the approximated AVO curves for the example.



It will be seen that the reflection curves arising from the top and bottom of the water-bearing sands suggest that zero reflectivity occurs at angles of incidence varying from about 39 degrees for low velocity sands to about 46 degrees for high velocity sands. Another way of envisaging the Fluid Factor is: a trace showing the reflectivity at that angle of incidence where water-bearing rocks are expected to show zero reflectivity. This angle is here named the Fluid Factor Angle, or  $\theta_f$ .

$$\text{Fluid Factor} = A + B \sin^2 \theta_f$$

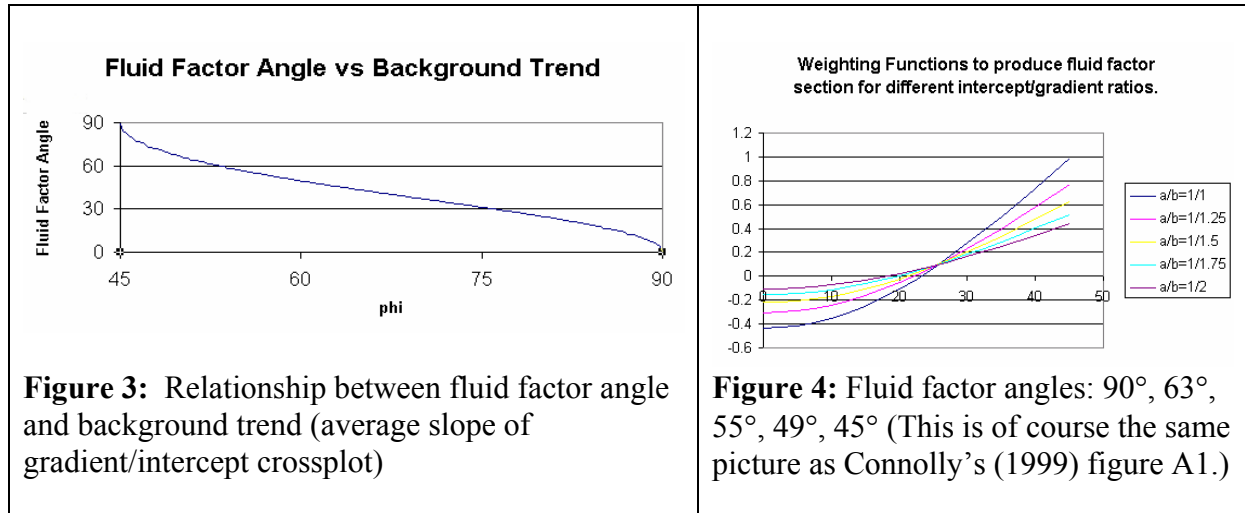
Figure 2 shows directly that for gas-bearing sands the Fluid Factor is negative at the top of the sands and positive at the bottom.

If the angle of incidence at the far trace of the seismic data is close to the Fluid Factor Angle, then the far angle stack will approximate a Fluid Factor section.

The two above definitions of the Fluid Factor (remembering that seismic data have no absolute units) are linked by the relation:

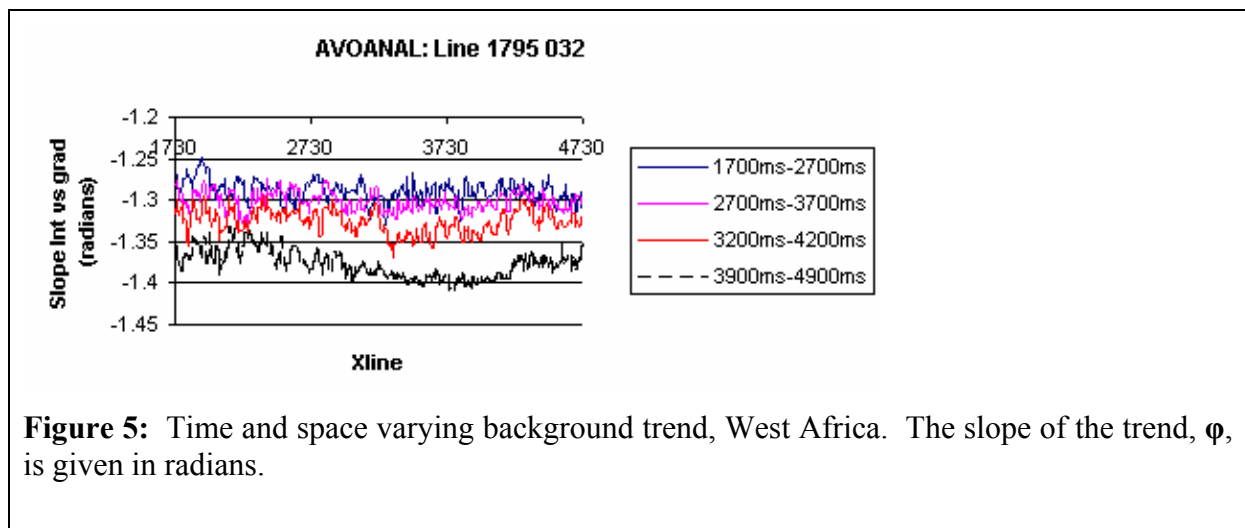
$$\cotan \phi = \sin^2 \theta_f \text{ This relationship is shown in figure 3.}$$

Figure 4 shows the weighting functions that will produce reflectivities at various angles of incidence. They can be inverted to Elastic Impedance as described by Conolly (1999). If the chosen angle is the Fluid Factor Angle, the result of the weighted stack will be the Fluid Factor section.



### The variability of background trends

Lastly, the time- and space-variant nature of background trends, whether defined by crossplot slope or Fluid Factor Angle, is illustrated in the data example of figure 5 from West Africa. If a Fluid Factor approach is to be optimal, it must comprehend these gradual trends.



### References:

- Castagna, J. P., Batzle, M. L., and Eastwood, R. L., 1985, Relationship between compressional- and shear-wave velocities in elastic silicate rocks: *Geophysics*, 50, 571-581.
- Castagna, J. P., and Smith, S. W., 1994, Comparison of AVO indicators: A modeling study: *Geophysics*, 59, 1849-1855.
- Connolly, P., 1999, Elastic impedance: *The Leading Edge*, 18, 438-452.
- Shuey, R. T., 1985, A simplification of the Zoeppritz equations: *Geophysics*, 50, 609-614.
- Smith, G. C., and Gidlow, P. M., 1987, Weighted stacking for rock property estimation and detection of gas: *Geophys. Prosp.*, 35, 993-1014.